Journal of Solid Mechanics Vol. 8, No. 4 (2016) pp. 806-822

Effects of Gravitational and Hydrostatic Initial Stress on a Two-Temperature Fiber-Reinforced Thermoelastic Medium for Three-Phase-Lag

S.M. Said [1,*] , M.I.A. Othman [2]

[1]*Department of Mathematics, Faculty of Science and Arts, Al-mithnab, Qassim University, P.O. Box 931, Buridah 51931, Al-mithnab, Kingdom of Saudi Arabia*
[2]*Department of Mathematics, Faculty of Science, Taif University 888, Saudi Arabia*

Received 26 July 2016; accepted 30 September 2016

ABSTRACT

The three-phase-lag model and Green–Naghdi theory without energy dissipation are employed to study the deformation of a two-temperature fiber-reinforced medium with an internal heat source that is moving with a constant speed under a hydrostatic initial stress and the gravity field. The modulus of the elasticity is given as a linear function of the reference temperature. The exact expressions for the displacement components, force stresses, thermal temperature and conductive temperature are obtained by using normal mode analysis. The variations of the considered variables with the horizontal distance are illustrated graphically. A comparison is made with the results of the two theories for two different values of a hydrostatic initial stress. Comparisons are also made with the results of the two theories in the absence and presence of the gravity field as well as the linear temperature coefficient.

Keywords : Fiber-reinforced; Gravity field; Green-Naghdi theory; Hydrostatic initial stress; Three-phase-lag model; Two-temperature.

1 INTRODUCTION

A theory of the heat conduction in deformable bodies which depends upon two distinct temperatures, the conductive temperature and the thermodynamic temperature, has been established by Chen and Gurtin [1] and Chen et al. [2, 3]. In time-independent problems, the difference between these two distinct temperatures is proportional to the heat supply and in the absence of any heat supply, these two-temperature are identical as Chen et al. [2]. For time-dependent situations and for wave propagation problems, in particular, the two-temperature are in general different, regardless of the presence of a heat supply. Warren and Chen [4] investigated the wave propagation in the two-temperature theory of thermoelasticity. Youssef [5] has proposed a theory in the context of the generalized theory of thermoelasticity with two-temperature. The propagation of harmonic plane waves in the media described by the two-temperature theory of thermoelasticity is investigated by Puri and Jordan [6]. Several problems with the two-temperature theory of thermoelasticity has been solved by Abbas and Youssef [7], Kumar and Mukhopadhyay [8], Das and Kanoria [9], Abbas and Zenkour [10], Othman et al. [11], and Zenkour and Abouelregal [12] etc.

Biot [13] formulated the coupled thermoelasticity theory to eliminate the paradox inherent in the classical uncoupled theory that the elastic deformation has no effect on the temperature. The field equations for the both theories are of a mixed parabolic-hyperbolic type, which predict infinite speeds for thermoelastic singles, contrary to physical observations. During the last three decades, generalized theories involving a finite speed of heat

*Corresponding author.
E-mail address: samia_said59@yahoo.com (S.M.Said).

transportation (hyperbolic heat transport equation) in elastic solids have been developed to remove this paradox. The first generalization is proposed by Lord and Shulman [14] and is known as the extended thermoelasticity theory which involves one thermal relaxation time parameter (single-phase-lag model). The second generalization of the coupled thermoelasticity theory is developed by Green and Lindsay [15], which involving two thermal relaxation time is known as temperature rate dependent thermoelasticity. The third generalization is known as low-temperature thermoelasticity introduced by Hetnarski and Ignaczak [16] called H–I theory. The fourth generalization is concerned with the thermoelasticity without energy dissipation and thermoelasticity with energy dissipation introduced by Green and Naghdi [17–19] and provide sufficient basic modifications in the constitutive equations that permit treatment of a much wider class of heat flow problems, labeled as types I, II, III. The nature of these three types of constitutive equations is such that when the respective theories are linearized, type-I is the same as the classical heat equation, whereas the linearized versions of type-II and type-III theories permit the propagation of thermal waves at a finite speed. The fifth generalization of the thermoelasticity theory is known as the dual-phase-lag thermoelasticity developed by Tzou [20] and Chandrasekhariah [21]. Tzou considered micro-structural effects in the delayed response in time in the macroscopic formulation by taking into account that increase of the lattice temperature is delayed due to photon-electron interactions on the macroscopic level. Tzou [20] introduced two-phase-lag to both the heat flux vector and the temperature gradient. According to this model, classical Fourier's law $q = -K\nabla T$ has been replaced by $\mathrm{q}(\mathrm{P},\mathrm{t}+\tau_{\mathrm{q}}) = -K\nabla T(\mathrm{P},\mathrm{t}+\tau_{\mathrm{T}})$, where the temperature gradient ∇T at a point P of the material at time $\mathrm{t}+\tau_{\mathrm{T}}$ corresponds to the heat flux vector q at the same point in time $\mathrm{t}+\tau_{\mathrm{q}}$. Here K is the thermal conductivity of the material. The delay time τ_{T} is interpreted as that caused by the micro-structural interactions and is called the phase-lag of the temperature gradient. The other delay time τ_{q} is interpreted as the relaxation time due to the fast transient effects of thermal inertia and is called the phase-lag of the heat flux. Recently Roy Choudhuri [22] has proposed a theory with three-phase-lag (3PHL) which is able to contain all the previous theories at the same time. In this case Fourier's law $q = -K\nabla T$ has been replaced by $\mathrm{q}(\mathrm{P},\mathrm{t}+\tau_{\mathrm{q}}) = -[K\nabla T(\mathrm{P},\mathrm{t}+\tau_{\mathrm{T}}) + K^{*}\nabla\nu(\mathrm{P},\mathrm{t}+\tau_{\nu})]$, where $\nabla\nu\,(\dot{\nu}=T)$ is the thermal displacement gradient and K^{*} is the additional material constant and τ_{ν} is the phase-lag for the thermal displacement gradient. The purpose of the work of Roy Choudhuri [22] was to establish a mathematical model that includes (3PHL) in the heat flux vector, the temperature gradient and in the thermal displacement gradient. For this model, we can consider several kinds of Taylor approximations to recover the previously cited theories. In particular the models of Green and Naghdi are recovered. Quintanilla and Racke [23] are introduced a note on the stability in the 3PHL heat conduction. Kar and Kanoria [24] studied a thermo-visco-elastic problem of a spherical shell in the context of the (3PHL) model. Quintanilla [25] discussed the spatial behavior of solutions of the (3PHL) heat equations. Abbas [26] discussed the (3PHL) model of a thermoelastic interaction in an unbounded fiber-reinforced anisotropic medium with a cylindrical cavity. The two-dimensional problem of a magneto-thermoelastic fiber-reinforced medium under temperature dependent properties with the (3PHL) model was presented by Othman and Said [27]. A domain of influence theorem for thermoelasticity with three-phase-lag model was discussed by Kumar and Kumar [28].

The thermal stresses in a material with the temperature-dependent properties are studied extensively by Noda [29]. Material properties such as the modulus of the elasticity and thermal conductivity vary with the temperature. When the temperature variation from the initial is not varying high, the properties of materials are constants. In the refractory industries, the structural components are exposed to high temperature change. In this case, neglecting the temperature dependence material properties will be due to errors as Jin and Batra [30]. Othman et al. [31–34] studied the two dimensional problem of the generalized thermoelasticity with the temperature dependent elastic moduli for the different theories. Fractional order theory of thermoelasticity for elastic medium with temperature dependent properties is discussed by Wang et al. [35].

In the present study, we shall formulate the two-temperature fiber-reinforced medium with the temperature dependent properties and with an internal heat source that is moving with a constant speed under the effect of a hydrostatic initial stress and the gravity field, then solve for the displacement components, force stresses, thermal temperature and conductive temperature. Normal mode analysis is used to obtain the exact expressions for the considered variables. A comparison is carried out between the considered variables as calculated from generalized thermoelasticity based on the (3PHL) and thermoelasticity without energy dissipation (G-N II) theory for two different values of a hydrostatic initial stress. Comparisons are also made with the results of the two theories in the absence and presence of the gravity field as well as the linear temperature coefficient.

2 FORMULATION OF THE PROBLEM AND BASIC EQUATIONS

We consider the problem of a thermoelastic half-space $(x \geq 0)$. The surface of a half-space is subjected to a thermal shock which is a function of *y* and *t*. We are interested in a plane strain in the *xy*-plane with displacement vector $\underline{u} = (u, v, 0)$. When all body forces are neglected, under the influence of the gravitational field and a hydrostatic initial stress the governing equations are:

(i) The stress-strain relation may be written as Belfield et al. [36] and Montanaro [37]

$$\sigma_{ij} = \lambda e_{kk}\delta_{ij} + 2\mu_T e_{ij} + \alpha(a_k a_m e_{km}\delta_{ij} + a_i a_j e_{kk}) + 2(\mu_L - \mu_T)(a_i a_k e_{kj} + a_j a_k e_{ki}) + \beta a_k a_m e_{km} a_i a_j - \gamma \hat{T}\delta_{ij} - P(\omega_{ij} + \delta_{ij}), \tag{1}$$

$$\omega_{ij} = \frac{1}{2}(u_{j,i} - u_{i,j}), \quad e_{ij} = \frac{1}{2}(u_{i,j} + u_{j,i}), \quad e_{kk} = e = \underline{\nabla}.\underline{u} = \frac{\partial u}{\partial x} + \frac{\partial v}{\partial y}. \qquad i, j = x, y. \tag{2}$$

where σ_{ij}'s are the components of stress, e_{ij}'s are the components of strain, e_{kk} is the dilatation, λ, μ_T's are the elastic constants, $\alpha, \beta, (\mu_L - \mu_T)$ are reinforcement parameters, $\gamma = (3\lambda + 2\mu)\alpha_t, \alpha_t$ is the thermal expansion coefficient, δ_{ij} is the Kronecker delta, *P* is the initial pressure, $\hat{T} = T - T_0$, where *T* is the temperature above the reference temperature T_0, and $\underline{a} \equiv (a_1, a_2, a_3), a_1^2 + a_2^2 + a_3^2 = 1.$ We choose the fiber-direction as $\underline{a} \equiv (1, 0, 0)$. Eq. (1) then yields

$$\sigma_{xx} = A_{11}u_{,x} + A_{12}v_{,y} - \gamma\hat{T} - P, \tag{3}$$

$$\sigma_{yy} = A_{12}u_{,x} + A_{22}v_{,y} - \gamma\hat{T} - P, \tag{4}$$

$$\sigma_{xy} = S_1 u_{,y} + S_2 v_{,x}, \quad \sigma_{yx} = S_2 u_{,y} + S_1 v_{,x}, \quad \sigma_{xz} = \sigma_{yz} = 0, \tag{5}$$

where $A_{11} = \lambda + 2(\alpha + \mu_T) + 4(\mu_L - \mu_T) + \beta, \quad A_{12} = \lambda + \alpha, \quad A_{22} = \lambda + 2\mu_T, \quad S_1 = \mu_L + \frac{P}{2}, \quad S_2 = \mu_L - \frac{P}{2}.$

In the above equations, we assume that as Othman and Said [27] $\lambda = \lambda_1(1 - \theta_0 T_0), \ \mu = \mu_1(1 - \theta_0 T_0), \ \alpha = \alpha_1(1 - \theta_0 T_0), \ \beta = \beta_1(1 - \theta_0 T_0), \quad \mu_L = \mu_{L1}(1 - \theta_0 T_0), \quad \mu_T = \mu_{T1}(1 - \theta_0 T_0),$ where $\lambda_1, \mu_1, \alpha_1, \beta_1, \mu_{L1}, \mu_{T1}$ are constants of the material and θ_0 is the linear temperature coefficient.

(ii) The dynamical equations of a fiber-reinforced thermoelastic medium is given by Othman et al. [34]

$$\rho\ddot{u}_i = \sigma_{ij,j} + F_i, \qquad i, j = 1, 2 \tag{6}$$

where F_i is the force due to the gravity field and is given in the form,

$$F_1 = \rho g\frac{\partial v}{\partial x}, \qquad F_2 = -\rho g\frac{\partial u}{\partial x}. \tag{7}$$

Introducing Eqs. (3)-(5) and (7) in Eq. (6) and using the summation convection, we note that the third equation of motion in (6) is identically satisfied and the first two equations become

$$\rho\frac{\partial^2 u}{\partial t^2} = A_{11}\frac{\partial^2 u}{\partial x^2} + B_2\frac{\partial^2 v}{\partial x \partial y} + S_1\frac{\partial^2 u}{\partial y^2} - \gamma\frac{\partial \hat{T}}{\partial x} + \rho g\frac{\partial v}{\partial x}, \tag{8}$$

$$\rho\frac{\partial^2 v}{\partial t^2}=A_{22}\frac{\partial^2 v}{\partial y^2}+B_2\frac{\partial^2 u}{\partial x\partial y}+S_1\frac{\partial^2 v}{\partial x^2}-\gamma\frac{\partial \hat{T}}{\partial y}-\rho g\frac{\partial u}{\partial x}, \tag{9}$$

where $B_2=S_2+A_{12}$.

(iii) The generalized heat conduction equation in the 3PHL model in the context of the two- temperature is given by Youssef [5] and Roy Choudhuri [22]

$$K^*\nabla^2\Phi+\tau_v^*\nabla^2\dot{\Phi}+K\tau_T\nabla^2\ddot{\Phi}=\left(1+\tau_q\frac{\partial}{\partial t}+\frac{1}{2}\tau_q^2\frac{\partial^2}{\partial t^2}\right)(\rho C_E\ddot{T}+\gamma T_0\,\ddot{e}-Q). \tag{10}$$

The relation between the conductive temperature and the thermodynamic temperature is

$$\Phi-T=\delta\Phi_{,ii}, \tag{11}$$

where K^* is the additional material constant, K is the coefficient of thermal conductivity, ρ is the mass density, C_E is the specific heat at constant strain, Φ is the conductive temperature, Q is a moving internal heat source, $\delta>0$ a constant called two-temperature parameter, τ_{T} and τ_{q} are the phase-lag of temperature gradient and the phase-lag of heat flux respectively. Also $\tau_v^*=\mathrm{K}+\tau_v\mathrm{K}^*$, where τ_v is the phase-lag of thermal displacement gradient. Eqs. (8)-(10), when $\mathrm{K}=\tau_{\mathrm{T}}=\tau_{\mathrm{q}}=\tau_v=0$, reduce to the equations of thermoelasticity without energy dissipation (GN-II) theory. In the above equations a dot denotes partial derivative with respect to time, and a comma followed by a subscript denotes partial derivative with respect to the corresponding coordinates.

Introducing the following non-dimensional quantities:

$$\begin{gathered}(\mathrm{x}',\mathrm{y}',\mathrm{u}',\mathrm{v}')=\mathrm{c}_1\eta(\mathrm{x},\mathrm{y},\mathrm{u},\mathrm{v}),\qquad(\mathrm{t}',\tau_{\mathrm{q}}',\tau_v',\tau_{\mathrm{T}}')=\mathrm{c}_1^2\eta(\mathrm{t},\tau_{\mathrm{q}},\tau_v,\tau_{\mathrm{T}}),\qquad \mathrm{g}'=\frac{\mathrm{g}}{\eta\,\mathrm{c}_1^3},\qquad \sigma_{\mathrm{ij}}'=\frac{\sigma_{\mathrm{ij}}}{\mu_{\mathrm{T}}},\\ \theta=\frac{\gamma\hat{\mathrm{T}}}{(\lambda+2\mu_{\mathrm{T}})},\qquad \Phi'=\frac{\gamma\,(\Phi-\mathrm{T}_0)}{(\lambda+2\mu_{\mathrm{T}})},\qquad \mathrm{P}'=\mathrm{P},\qquad \mathrm{Q}'=\frac{\gamma\mathrm{Q}}{\rho\,\mathrm{C}_{\mathrm{E}}\,\mathrm{c}_1^4\,\eta^2(\lambda+2\mu_{\mathrm{T}})},\qquad \mathrm{i},\mathrm{j}=1,2.\end{gathered} \tag{12}$$

where $\eta=\dfrac{\rho\mathrm{C}_{\mathrm{E}}}{\mathrm{K}^*}$, $\mathrm{c}_1^2=\dfrac{(\lambda+2\mu_{\mathrm{T}})}{\rho}$.

Using the above non-dimensional variables defined in Eq. (12), the above governing equations take the following form (dropping the primes for convenience)

$$\frac{\partial^2\mathrm{u}}{\partial\mathrm{t}^2}=\mathrm{h}_{11}\frac{\partial^2\mathrm{u}}{\partial\mathrm{x}^2}+\mathrm{h}_2\frac{\partial^2\mathrm{v}}{\partial\mathrm{x}\partial\mathrm{y}}+\mathrm{h}_1\frac{\partial^2\mathrm{u}}{\partial\mathrm{y}^2}-\frac{\partial\theta}{\partial\mathrm{x}}+\mathrm{g}\frac{\partial\mathrm{v}}{\partial\mathrm{x}}, \tag{13}$$

$$\frac{\partial^2\mathrm{v}}{\partial\mathrm{t}^2}=\mathrm{h}_{22}\frac{\partial^2\mathrm{v}}{\partial\mathrm{y}^2}+\mathrm{h}_2\frac{\partial^2\mathrm{u}}{\partial\mathrm{x}\partial\mathrm{y}}+\mathrm{h}_1\frac{\partial^2\mathrm{v}}{\partial\mathrm{x}^2}-\frac{\partial\theta}{\partial\mathrm{y}}-\mathrm{g}\frac{\partial\mathrm{u}}{\partial\mathrm{x}}, \tag{14}$$

$$\mathrm{C}_{\mathrm{K}}\Phi_{,\mathrm{ii}}+\mathrm{C}_v\dot{\Phi}_{,\mathrm{ii}}+\mathrm{C}_{\mathrm{T}}\ddot{\Phi}_{,\mathrm{ii}}=\left(1+\tau_{\mathrm{q}}\frac{\partial}{\partial\mathrm{t}}+\frac{1}{2}\tau_{\mathrm{q}}^2\frac{\partial^2}{\partial\mathrm{t}^2}\right)(\ddot{\theta}+\varepsilon\,\ddot{\mathrm{e}}-\mathrm{Q}), \tag{15}$$

$$\Phi-\theta=\beta_0\,\Phi_{,\mathrm{ii}}, \tag{16}$$

where $(h_1, h_2, h_{11}, h_{22}) = \frac{(S_1, B_2, A_{11}, A_{22})}{\rho c_1^2}$, $C_K = \frac{K^*}{\rho C_E c_1^2}$, $C_\nu = \frac{\eta K}{\rho C_E} + C_K \tau_\nu$, $C_T = \frac{\eta K \tau_T}{\rho C_E}$, $\beta_0 = \delta c_1^2 \eta^2$, $\varepsilon = \frac{\gamma^2 T_0}{\rho C_E (\lambda + 2\mu_T)}$.

3 NORMAL MODE ANALYSIS

The solution of the considered physical variable can be decomposed in terms of normal mode as the following form:

$$\begin{aligned} &[u, v, \theta, \Phi, \sigma_{ij}](x, y, t) = [u^*, v^*, \theta^*, \Phi^*, \sigma_{ij}^*](x) \exp(\omega t + i m y), \\ &Q = Q^* \exp(\omega t + i m y), \qquad Q^* = Q_0 V_0, \end{aligned} \tag{17}$$

where ω is a complex constant, $i = \sqrt{-1}$, m is the wave number in the *y*-direction, and $u^*(x), v^*(x), \theta^*(x), \Phi^*(x), \sigma_{ij}^*(x)$ are the amplitudes of the field quantities.

Introducing Eq. (17) in Eqs. (13)-(16), we get

$$[h_{11} D^2 - N_1] u^* + C_1 D v^* = D\theta^*, \tag{18}$$

$$C_2 D u^* + [h_1 D^2 - N_2] v^* = i m \theta^*, \tag{19}$$

$$\varepsilon N_3 D u^* + i \varepsilon m N_3 v^* + N_3 \theta^* = [N_4 D^2 - N_5] \Phi^* + N_0 Q_0 V_0, \tag{20}$$

$$\theta^* = (N_8 - \beta_0 D^2) \Phi^*, \tag{21}$$

where,

$$N_1 = \omega^2 + h_1 m^2, \quad C_1 = i m h_2 + g, \quad C_2 = i m h_2 - g, \quad N_2 = \omega^2 + h_{22} m^2, \quad N_3 = \omega^2 (1 + \tau_q \omega + \frac{1}{2} \tau_q^2 \omega^2),$$

$$N_4 = C_K + C_\nu \omega + C_T \omega^2, \quad N_5 = N_4 m^2, \quad N_0 = 1 + \tau_q \omega + \frac{1}{2} \tau_q^2 \omega^2, \quad N_8 = 1 + \beta_0 m^2.$$

Introducing Eq. (21) in Eqs. (18)-(20), we get

$$[h_{11} D^2 - N_1] u^* + C_1 D v^* = D(N_8 - \beta_0 D^2) \Phi^*, \tag{22}$$

$$C_2 D u^* + [h_1 D^2 - N_2] v^* = i m (N_8 - \beta_0 D^2) \Phi^*, \tag{23}$$

$$\varepsilon N_3 D u^* + i \varepsilon m N_3 v^* = [N_6 D^2 - N_7] \Phi^* + N_0 Q_0 V_0, \tag{24}$$

where $N_6 = \beta_0 N_3 + N_4$, $N_7 = N_3 N_8 + N_5$, $D = \frac{d}{dx}$.

Eliminating $v^*(x)$ and $\Phi^*(x)$ between Eqs. (22)-(24), we obtain the sixth-order ordinary differential equation satisfied with $u^*(x)$,

$$[D^6 - L D^4 + L_1 D^2 - L_2] u^*(x) = 0, \tag{25}$$

where,

$$L = \frac{L_4}{L_3}, \quad L_1 = \frac{L_5}{L_3}, \quad L_2 = \frac{L_6}{L_3}, \quad L_3 = (h_{11} N_6 + \varepsilon N_3 \ \beta_0) h_1,$$

$$L_4 = C_1 C_2 N_6 + \varepsilon N_3 N_2 \beta_0 + \varepsilon N_3 N_8 h_1 + N_1 N_6 h_1 + N_7 h_1 h_{11} + N_2 N_6 h_{11} + m^2 \varepsilon \beta_0 N_3 h_{11} - 2m^2 \varepsilon N_3 \beta_0 h_2,$$

$$L_5 = C_1 C_2 N_7 + \varepsilon N_3 N_8 N_2 + N_1 N_2 N_6 + N_1 N_7 h_1 + m^2 \varepsilon N_1 N_3 \beta_0 + N_2 N_7 h_{11} + m^2 \varepsilon N_3 N_8 h_{11} - 2m^2 \varepsilon N_3 N_8 h_2,$$

$$L_6 = N_1 N_2 N_7 + m^2 \varepsilon N_3 N_8 N_1.$$

Eq. (25) can be factored as:

$$(\mathrm{D}^2 - k_1^2)(\mathrm{D}^2 - k_2^2)(\mathrm{D}^2 - k_3^2)\ u^*(x) = 0, \tag{26}$$

where k_n^2 $(n = 1, 2, 3)$ are the roots of the characteristic equation of Eq. (25). The solution of Eq. (25), which is bound as $x \to \infty$, is given by

$$u^*(x) = \sum_{n=1}^{3} G_n \exp(-k_n x). \tag{27}$$

Similarly,

$$v^*(x) = \sum_{n=1}^{3} R_{1n} G_n \exp(-k_n x) - \frac{\mathrm{i}m N_0 \ N_1 N_8 \ Q_0 V_0}{L_2 L_3}, \tag{28}$$

$$\Phi^*(x) = \sum_{n=1}^{3} R_{2n} G_n \exp(-k_n x) + \frac{N_1 N_2 \ N_0 \ Q_0 V_0}{L_2 L_3}, \tag{29}$$

where

$$R_{1n} = \frac{\mathrm{i}mN_1 - (\mathrm{i}mh_{11} - C_2)k_n^2}{h_1 k_n^3 - (N_2 + imC_1)k_n}, \qquad R_{2n} = \frac{-N_1 + h_{11}k_n^2 - C_1 k_n R_{1n}}{-N_8 k_n + \beta_0 k_n^3}.$$

Introducing Eq. (29) in Eq. (21), we have

$$\theta^*(x) = \sum_{n=1}^{3} R_{3n} G_n \exp(-k_n x) + \frac{N_1 N_2 \ N_8 N_0 \ Q_0 V_0}{L_2 L_3}, \tag{30}$$

where, $R_{3n} = (N_8 - \beta_0 k_n^2) R_{2n}$.

Using Eqs. (12) and (17) in Eqs. (3) and (5), we obtain

$$\sigma_{xx}^* = \frac{1}{\mu_T}[A_{11}\mathrm{D}u^* + \mathrm{i}mA_{12}v^* - (\lambda + 2\mu_T)\theta^* - P^*], \tag{31}$$

$$\sigma_{xy}^* = \frac{1}{\mu_T}[\mathrm{i}mS_1 u^* + S_2 \mathrm{D}v^*], \qquad \sigma_{yx}^* = \frac{1}{\mu_T}[\mathrm{i}mS_2 u^* + S_1 \mathrm{D}v^*]. \tag{32}$$

Introducing Eqs. (27), (28) and (30) in Eqs. (31) and (32), this yields

$$\sigma_{xx}^*(x) = \sum_{n=1}^{3} R_{4n} G_n \exp(-k_n x) + r_1, \tag{33}$$

$$\sigma_{xy}^{*}(x)=\sum_{n=1}^{3}R_{5n}G_n\exp(-k_n x),\qquad \sigma_{yx}^{*}(x)=\sum_{n=1}^{3}R_{6n}G_n\exp(-k_n x), \tag{34}$$

where

$$P^{*}=P\exp[-(\omega t+\mathrm{i}my)],\qquad R_{4n}=\frac{1}{\mu_T}[-A_{11}k_n+\mathrm{i}mA_{12}R_{1n}-(\lambda+2\mu_T)R_{3n}],\quad R_{5n}=\frac{1}{\mu_T}[\mathrm{i}mS_1-S_2\,k_n\,R_{1n}],$$

$$R_{6n}=\frac{1}{\mu_T}[\mathrm{i}mS_2-S_1\,k_n\,R_{1n}],\quad r_1=\frac{[m^2A_{12}-(\lambda+2\mu_T)N_2]N_1\,N_0\,N_8\,Q_0V_0}{\mu_T\,L_3\,L_2}-\frac{P^{*}}{\mu_T}.$$

4 APPLICATION (THERMAL SHOCK PROBLEM)

In this section we determine the parameters $G_n(n=1,2,3)$. In the physical problem, we should suppress the positive exponentials that are unbounded at infinity. The constants G_1, G_2, G_3 have to be chosen such that the boundary conditions on the surface at $x=0$ take the form:

i) A thermal boundary condition that the surface of the half-space is subjected to a thermal insulated boundary

$$\frac{\partial\Phi}{\partial x}=0. \tag{35}$$

ii) A mechanical boundary condition that the surface of the half-space is subjected to a hydrostatic initial stress

$$\sigma_{xx}=f(y,t)=-R_P\,f^{*}\exp(\omega t+\mathrm{i}my) \tag{36}$$

iii) A mechanical boundary condition that the surface of the half-space is traction free

$$\sigma_{xy}(0,y,t)=0 \tag{37}$$

$f(y,t)$ is an arbitrary function of y,t,R_P is the magnitude of a hydrostatic initial stress, and f^{*} is a constant. Substituting the expressions of the variables considered into the above boundary conditions, we can obtain the following equations satisfied by the parameters:

$$-\sum_{n=1}^{3}k_nR_{2n}G_n=0,\quad \sum_{n=1}^{3}R_{4n}G_n=-R_Pf^{*}-r_1,\quad \sum_{n=1}^{3}R_{5n}G_n=0 \tag{38}$$

Solving the above system of Eqs. (38), we obtain a system of three equations. After applying the inverse of matrix method, we have the values of the three constants $G_n(n=1,2,3)$. Hence, we obtain the expressions of displacements, the thermal temperature, the conductive temperature and the stress components.

$$\begin{pmatrix}G_1\\G_2\\G_3\end{pmatrix}=\begin{pmatrix}k_1R_{21} & k_2R_{22} & k_3R_{23}\\ R_{41} & R_{42} & R_{43}\\ R_{51} & R_{52} & R_{53}\end{pmatrix}^{-1}\begin{pmatrix}0\\-R_Pf^{*}-r_1\\0\end{pmatrix} \tag{39}$$

5 SPECIAL CASES OF THERMOELASTIC THEORY AND PARTICULAR CASES

(i) The corresponding equations for a two-temperature fiber-reinforced generalized thermoelastic medium, in the presence of a hydrostatic initial stress $(R_P = 5)$ with temperature dependent properties $(\theta_0 = 0.003)$ in the absence of the gravity field from the above mentioned cases by taking $g = 0$.

(ii) The corresponding equations for a two-temperature fiber-reinforced generalized thermoelastic medium, in the presence of the gravity field $(g = 9.8)$ with temperature dependent properties $(\theta_0 = 0.003)$ for two different values of a hydrostatic initial stress from the above mentioned cases by taking $R_P = 5,12.$

(iii) The corresponding equations for a two-temperature fiber-reinforced generalized thermoelastic medium, in the presence of the gravity field $(g = 9.8)$ and a hydrostatic initial stress $(R_P = 5)$, without temperature dependent properties from the above mentioned cases by taking θ_0 to be vanishing.

(iv) Equations of the (3PHL) model when, $K, \tau_T, \tau_q, \tau_v > 0$ and the solutions are always (exponentially) stable if $\frac{2K\tau_T}{\tau_q} > \tau_v^* > K^*\tau_q$ as in Quintanilla and Racke [24].

(v) Equations of the (GN-II) theory when, $K = \tau_T = \tau_q = \tau_v = 0$.

6 NUMERICAL RESULTS AND DISCUSSION

In order to illustrate the theoretical results obtained in the preceding section, and to compare these in the context of the (3PHL) model and the (GN-II) theory, we now present some numerical results for the physical constants as Othman and Said [27].

$\lambda_1 = 7.59\text{x}10^{10}\,\text{N.m}^{-2}$, $\mu_{T1} = 9.89\text{x}10^{8}\,\text{N.m}^{-2}$, $\mu_{L1} = 2.45\text{x}10^{10}\,\text{N.m}^{-2}$, $\rho = 7800\,\text{kg.m}^{-3}$, $m = 1.2$, $f^* = 1$, $a_1 = -1.28\text{x}10^{10}\,\text{N.m}^{-2}$,
$\beta_1 = 0.32\text{x}10^{10}\,\text{N.m}^{-2}$, $C_E = 383.1\,\text{J.kg}^{-1}.\text{K}^{-1}$, $\tau_T = 0.007\,\text{s}$, $\tau_q = 0.009\,\text{s}$, $\tau_v = 0.006\,\text{s}$, $T_0 = 273\,\text{K}$, $K^* = 386\,\text{w.s}^{-1}.\text{m}^{-1}.\text{K}^{-1}$,
$\mu_1 = 1.89\text{x}10^{10}\,\text{kg.m}^{-1}.\text{s}^{-2}$, $K = 800\,\text{w.m}^{-1}.\text{K}^{-1}$, $\omega = \omega_0 + i\xi$, $\omega_0 = -0.2$, $\xi = 0.9$, $P = 9.5\text{x}10^{8}\,\text{N.m}^{-2}$, $g = 9.8\,\text{m.s}^{-2}$, $R_P = 5,12\,\text{N.m}^{-2}$,
$\delta = 1.5\text{x}10^{-14}$, $a_1 = 5.78\text{x}10^{-3}\,\text{K}^{-1}$, $\theta_0 = 0.003\,\text{K}^{-1}$, $Q_0 = 6\text{K}$, $V_0 = 0.5\,\text{m.s}^{-1}$.

The computations were carried out for a value of time $t = 1.3$. The variations of the thermal temperature θ, the conductive temperature Φ, the displacement components u,v and the stress components $\sigma_{xx}, \sigma_{xy}, \sigma_{yx}$ with distance x in the plane $y = -0.2$ for the problem under consideration based on the (3PHL) model and the (GN-II) theory in the context of two-temperature. The results are shown in Figs. 1-21. The graphs show the four curves predicted by two different theories of thermoelasticity. In these figures, the solid lines represent the solution in the (3PHL) model and the dashed lines represent the solution derived using the (GN-II) theory. Here all the variables are taken in non-dimensional forms.

Figs. 1-7 show comparisons between the displacement components, the thermal temperature θ, the conductive temperature Φ, and the stress components $\sigma_{xx}, \sigma_{xy}, \sigma_{yx}$ with temperature dependent properties $(\theta_0 = 0.003)$ in the presence $(g = 9.8)$ and absence $(g = 0)$ of the gravity field with a hydrostatic initial stress $R_P = 5$.

Fig. 1 depicts that the distribution of the horizontal displacement *u* begins from a positive value in the presence of the gravity field, but it begins from a negative value in the absence of the gravity field. In the context of the two models and in the presence of the gravity field, *u* starts with increasing, then decreases and in last becomes nearly constant. However, the context of the two models and in the absence of the gravity field, *u* starts with increasing to a maximum value, then decreases, and again increases. Fig. 2 shows that the distribution of the vertical displacement *v* begins from a negative value in the presence of the gravity field, but it begins from a positive value in the absence of the gravity field. In the context of the two models and in the presence of the gravity field, *v* starts with decreasing, then increases, again decreases and in the last becomes nearly constant. However, in the context of the two theories and in the absence of the gravity field, *v* starts with decreasing to a minimum value, then increases, and in the last decreases. Fig. 3 exhibits the distribution of the conductive temperature Φ and demonstrates that it begins from negative values. In the context of the two models and in the presence of the gravity field, Φ starts with increasing to

a maximum value, then decreases, and in the last increases. However, in the context of the two models and in the absence of the gravity field, Φ starts with increasing, then decreases, again increases, and in the last becomes nearly constant. Fig. 4 describes that the distribution of the thermal temperature θ begins from negative values. In the context of the two models and in the presence of the gravity field, θ starts with decreasing to a minimum value, then increases to a maximum value, and also moves in a wave propagation. However, in the context of the two theories and in the absence of the gravity field, θ starts with increasing to a maximum value, then decreases, and in the last increases. Fig. 5 displays that the distribution of the stress component σ_{xx} begins from a negative value and satisfies the boundary condition at $x = 0$. In the context of the two models and in the presence of the gravity field, σ_{xx} starts with increasing to a maximum value, then decreases to a minimum value, and also moves in a wave propagation. However, in the context of the two models and in the absence of the gravity field, σ_{xx} starts with increasing to a maximum value, and then decreases to a minimum value, and in the last increases. Fig. 6 explains the distribution of the stress component σ_{xy} and demonstrates that it reaches a zero value and satisfies the boundary condition at $x = 0$. In the context of the two theories and in the presence of the gravity field, σ_{xy} starts with increasing, then decreases, and in the last becomes nearly constant. However, in the context of the two theories and in the absence of the gravity field, σ_{xy} starts with increasing to a maximum value, and then decreases to a minimum value, again increases, and in the last decreases. Fig. 7 depicts that the distribution of the stress component σ_{yx} begins from negative values. In the context of the two theories and in the presence of the gravity field, σ_{yx} starts with increasing, then decreases, again increases, and in the last becomes nearly constant. However, in the context of the two theories and in the absence of the gravity field, σ_{yx} starts with increasing to a maximum value, then decreases, and in the last increases. There is a significant difference in the result of σ_{xy} and σ_{yx} due to the presence of a hydrostatic initial stress. Figs. 1-7 demonstrate that the gravity field has a significant role on all the physical quantities and there no difference in the results between the two theories in the absence of the gravity field.

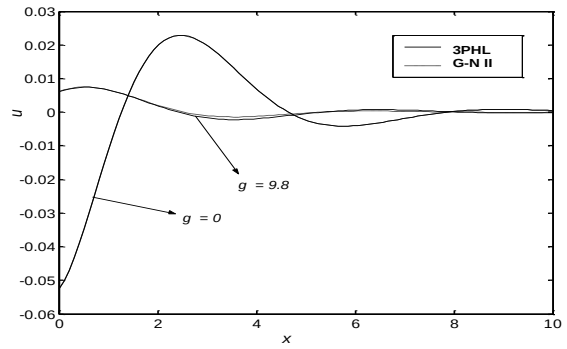

Fig.1
Horizontal displacement distribution *u* in the absence and presence of the gravity field.

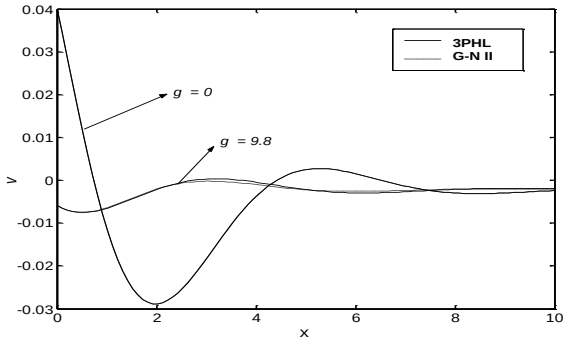

Fig.2
Vertical displacement distribution *v* in the absence and presence of the gravity field.

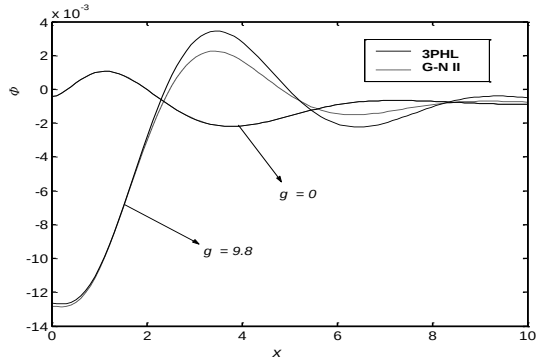

Fig.3
Conductive temperature distribution Φ in the absence and presence of the gravity field.

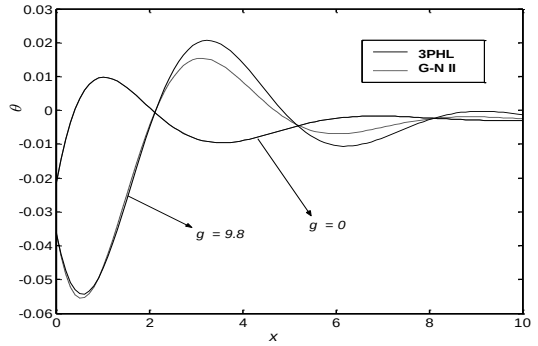

Fig.4
Thermal temperature distribution θ in the absence and presence of the gravity field.

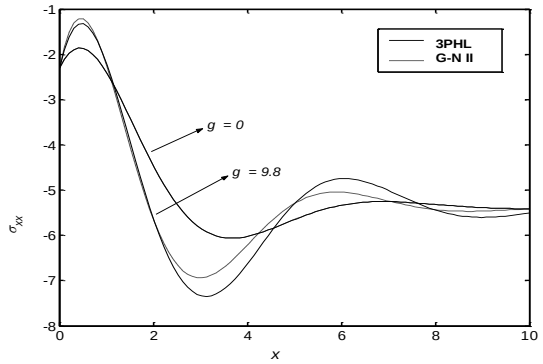

Fig.5
Distribution of stress component σ_{xx} in the absence and presence of the gravity field.

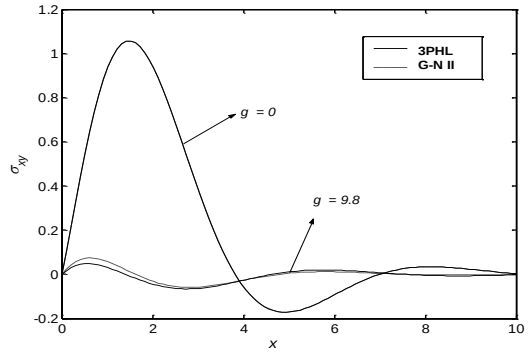

Fig.6
Distribution of stress component σ_{xy} in the absence and presence of the gravity field.

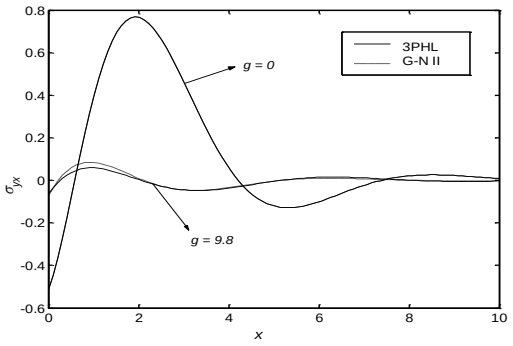

Fig.7
Distribution of stress component σ_{yx} in the absence and presence of the gravity field.

Figs. 8-14 show comparisons between the displacement components, the thermal temperature θ, the conductive temperature Φ, and the stress components σ_{xx}, σ_{xy}, σ_{yx} with temperature dependent properties $(\theta_0 = 0.003)$ for two different values of a hydrostatic initial stress $(R_P = 5,12)$ in the presence of gravity field $(g = 9.8)$.

Fig. 8 depicts that the distribution of the horizontal displacement *u* begins from positive values. In the context of the two models, *u* starts with increasing to a maximum value, then decreases to a minimum value, and also moves in a wave propagation for $R_P = 12$. Fig. 9 shows that the distribution of the vertical displacement *v* begins from negative values. In the context of the two models, *v* starts with decreasing to a minimum value, then increases to a maximum value, and also moves in a wave propagation for $R_P = 12$. Fig. 10 exhibits the distribution of the conductive temperature Φ and demonstrates that it begins from negative values. In the context of the two models, Φ starts with decreasing to a minimum value, then increases to a maximum value, and also moves in a wave propagation for $R_P = 12$. Fig. 11 describes that the distribution of the thermal temperature θ begins from negative values for $R_P = 5$, but it begins from positive values for $R_P = 12$. In the context of the two models, θ starts with decreasing to a minimum value, then increases to a maximum value, and also moves in a wave propagation for $R_P = 12$. Fig. 12 explains that the distribution of the stress component σ_{xx} begins from negative values and satisfies the boundary condition at $x = 0$. In the context of the two models, σ_{xx} starts with increasing to a maximum value, then decreases to a minimum value, and also moves in a wave propagation for $R_P = 12$. Fig. 13 displays the distribution of the stress component σ_{xy} and demonstrates that it reaches a zero value and satisfies the boundary condition at $x = 0$. In the context of the two theories, σ_{xy} starts with increasing to a maximum value, then decreases to a minimum value, and also moves in a wave propagation for $R_P = 12$. Fig. 14 depicts that the distribution of the stress component σ_{yx} begins from negative values. In the context of the two theories, σ_{yx} starts with increasing to a maximum value, then decreases, and also moves in a wave propagation for $R_P = 12$. Figs. 8-14 exhibit that the hydrostatic initial stress has an important effect on all the physical quantities.

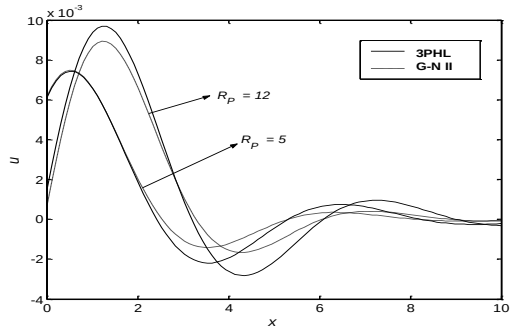

Fig.8
Horizontal displacement distribution *u* for two different values of a hydrostatic initial stress.

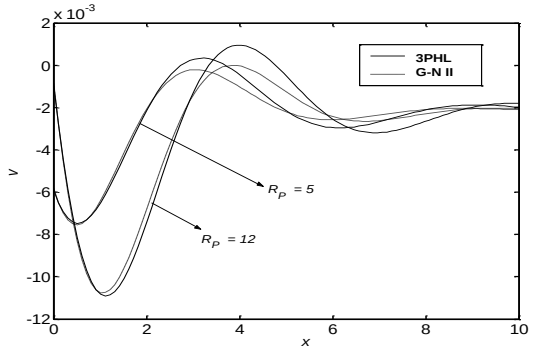

Fig.9
Vertical displacement distribution v for two different values of a hydrostatic initial stress.

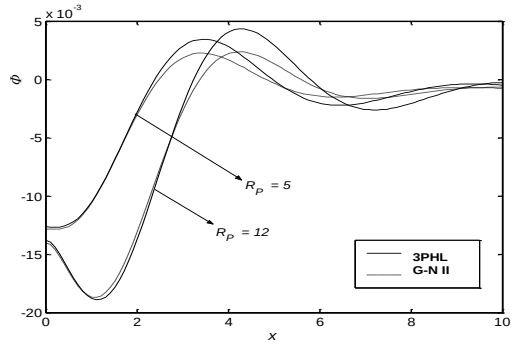

Fig.10
Conductive temperature distribution Φ for two different values of a hydrostatic initial stress.

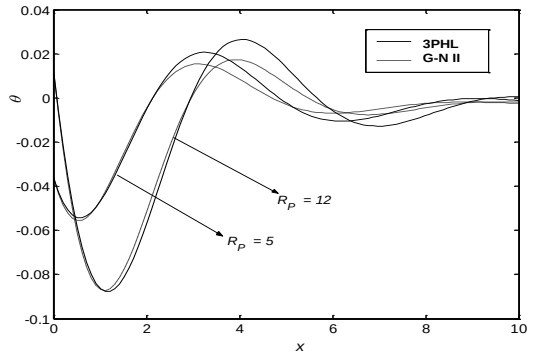

Fig.11
Thermal temperature distribution θ for two different values of a hydrostatic initial stress.

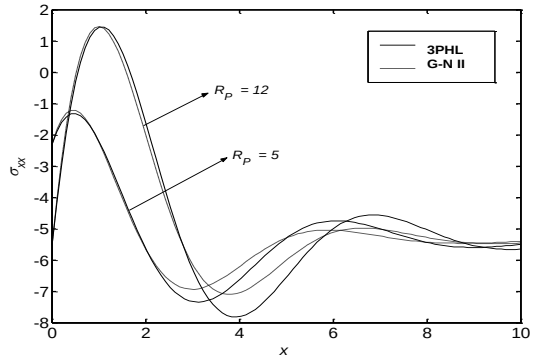

Fig.12
Distribution of stress component σ_{xx} for two different values of a hydrostatic initial stress.

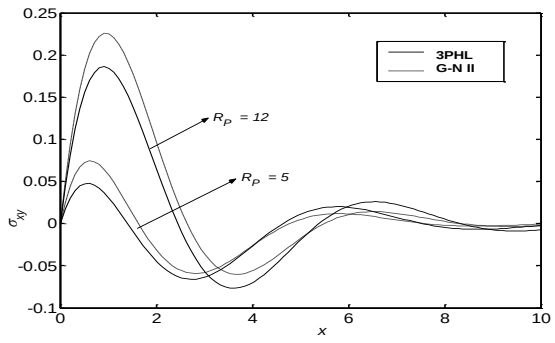

Fig.13
Distribution of stress component σ_{xy} for two different values of a hydrostatic initial stress.

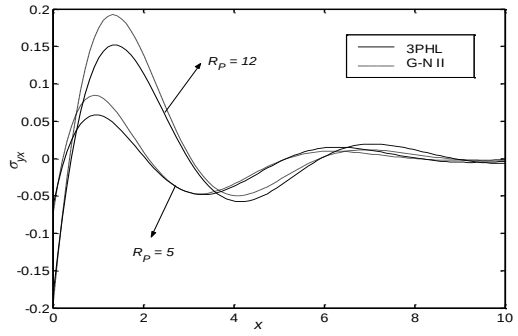

Fig.14
Distribution of stress component σ_{yx} for two different values of a hydrostatic initial stress.

Figs. 15-21 show comparisons between the displacement components u,v, the thermal temperature θ, the conductive temperature Φ, and the stress components $\sigma_{xx},\sigma_{xy},\sigma_{yx}$ in the presence of a hydrostatic initial stress $(R_P = 5)$ and the gravity field $(g = 9.8)$, with $(\theta_0 = 0.003)$ and without $(\theta_0 = 0)$ temperature dependent properties.

Fig. 15 depicts that the distribution of the horizontal displacement u begins from a positive value for $(\theta_0 = 0.003)$, but it begins from a negative value for $\theta_0 = 0$. In the context of the two models, u starts with increasing to a maximum value, then decreases, and in the last increases for $\theta_0 = 0$. Fig. 16 exhibits that the distribution of the vertical displacement v begins from a negative value for $(\theta_0 = 0.003)$, but it begins from a positive value for $\theta_0 = 0$. In the context of the two models, v starts with decreasing to a minimum value, then increases, and in the last decreases for $\theta_0 = 0$. Fig. 17 explains the distribution of the conductive temperature Φ and demonstrates that it begins from negative values. In the context of the two models, Φ starts with decreasing, then increases, and in the last becomes nearly constant for $\theta_0 = 0$. Fig. 18 describes that the distribution of the thermal temperature θ begins from a negative value for $(\theta_0 = 0.003)$, but it begins from a positive value for $\theta_0 = 0$. In the context of the two models, θ starts with decreasing to a minimum value, then increases, and in the last decreases for $\theta_0 = 0$. Fig. 19 explains that the distribution of the stress component σ_{xx} begins from a negative value and satisfies the boundary condition at $x = 0$. In the context of the two models, σ_{xx} starts with increasing to a maximum value, then decreases, and in the last becomes nearly constant for $\theta_0 = 0$. Fig. 20 exhibits the distribution of the stress component σ_{xy} and demonstrates that it reaches a zero value and satisfies the boundary condition at $x = 0$. In the context of the two theories, σ_{xy} starts with increasing to a maximum value, then decreases to a minimum value, and also moves in a wave propagation for $\theta_0 = 0$. Fig. 21 depicts that the distribution of the stress component σ_{yx} begins from negative values. In the context of the two theories, σ_{yx} starts with increasing to a maximum value, then decreases, and also moves in wave propagation for $\theta_0 = 0$. Figs. 15-21 exhibit that the linear temperature coefficient (θ_0) plays a significant role on all the physical quantities.

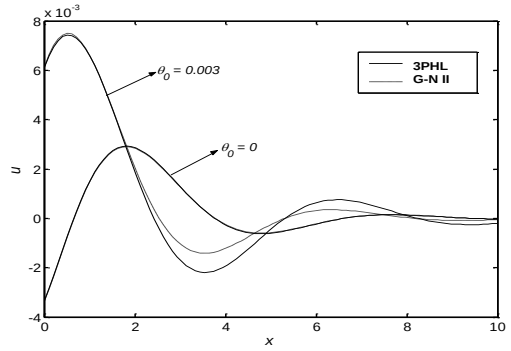

Fig.15
Horizontal displacement distribution u in the absence and presence of the linear temperature coefficient.

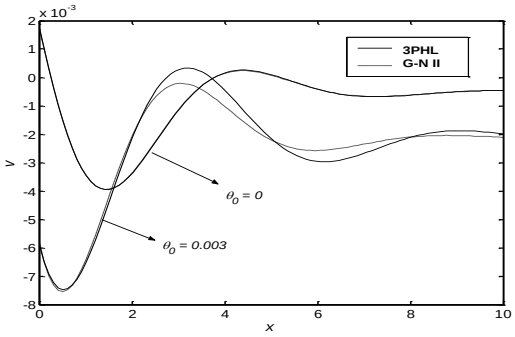

Fig.16
Vertical displacement distribution v in the absence and presence of the linear temperature coefficient.

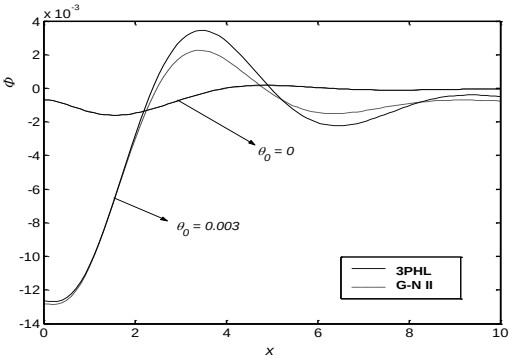

Fig.17
Conductive temperature distribution Φ in the absence and presence of the linear temperature coefficient.

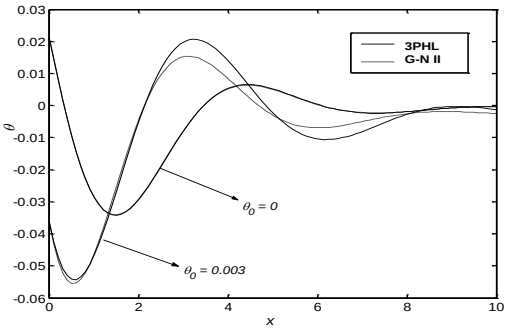

Fig.18
Thermal temperature distribution θ in the absence and presence of the linear temperature coefficient.

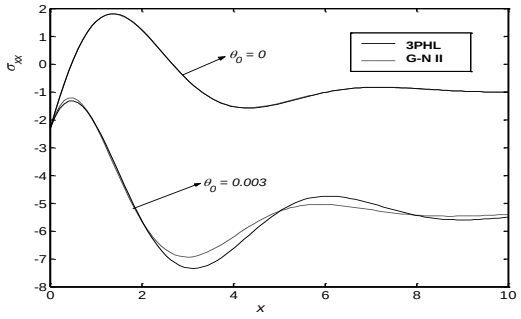

Fig.19
Distribution of stress component σ_{xx} in the absence and presence of the linear temperature coefficient.

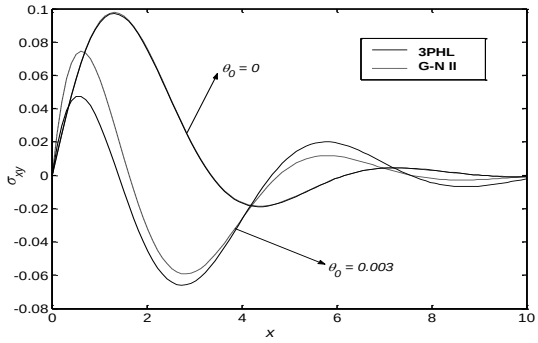

Fig.20
Distribution of stress component σ_{xy} in the absence and presence of the linear temperature coefficient.

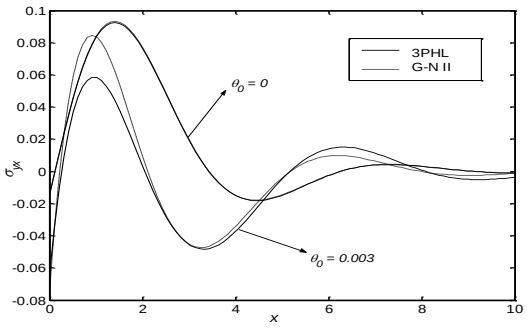

Fig.21
Distribution of stress component σ_{yx} in the absence and presence of the linear temperature coefficient.

7 CONCLUSIONS

By comparing the figures which obtained under the two thermoelastic theories, important phenomena are observed:

(1) Deformation of a body depends on the nature of the applied force as well as the type of boundary conditions.
(2) The method that was used in the present article is applicable to a wide range of problems in thermodynamics and thermoelasticity.
(3) Analytical solutions based upon normal mode analysis of the thermoelastic problem in solids have been developed and utilized.
(4) There are significant differences in the field quantities under the GN-II theory and the 3PHL model due to the phase-lag of temperature gradient and the phase-lag of heat flux.
(5) It is clear that the gravity field, a hydrostatic initial stress (R_P) and the linear temperature coefficient (θ_0) play significant roles on all the physical quantities.
(6) The 3PHL model is a mathematical model that includes the heat flux vector, the temperature gradient and the thermal displacement gradient, which are useful in the problems of heat transfer, heat conduction,

nuclear boiling, exothermic catalytic reactions, phonon-electron interactions, phonon-scattering. So the 3PHL model is the most adequate theory to describe the present problem.

(7) The curves in the context of the 3PHL model and the GN-II theory decrease exponentially with increasing *x*; this indicates that the thermoelastic waves are un attenuated and non-dispersive, while purely thermoelastic waves undergo both attenuation and dispersion.

REFERENCES

[1] Chen P.J., Gurtin M. E., 1968, On a theory of heat conduction involving two temperatures, *Zeitschrift für Angewandte Mathematik und Physik* **19**: 614-627.

[2] Chen P.J., Williams W.O., 1968, A note on non simple heat conduction, *Zeitschrift für angewandte Mathematik und Physik* **19**: 969-970.

[3] Chen P.J., Gurtin M. E., Williams W.O., 1969, On the thermodynamics of non-simple elastic materials with two-temperatures, *Zeitschrift für Angewandte Mathematik und Physik* **20**: 107-112.

[4] Warren W. E., Chen P. J., 1973, Wave propagation in the two temperatures theory of thermoelasticity, *Journal of Acta Mechcanica* **16**: 21-33.

[5] Youssef H. M., 2005, Theory of two-temperature generalized thermoelasticity, *Journal of Applied Mathematics* **71**: 383-390.

[6] Puri P., Jordan P.M., 2006, On the propagation of harmonic plane wanes under the two temperature theory, *International Journal of Engineering Science* **44**: 1113-1126.

[7] Abbas I. A., Youssef H. M., 2009, Finite element method of two-temperature generalized magneto-thermoelasticity, *Journal Archive of Applied Mechanics* **79**: 917-925.

[8] Kumar R., Mukhopadhyay S., 2010, Effects of thermal relaxation time on plane wave propagation under two-temperature thermoelasticity, *International Journal of Engineering Science* **48**: 128-139.

[9] Das P., Kanoria M., 2012, Two-temperature magneto-thermoelastic response in a perfectly conducting medium based on GN-III Model, *International Journal of Pure and Applied Mathematics* **81**: 199-229.

[10] Abbas I. A., Zenkour A. M., 2014, Two-temperature generalized thermoplastic interaction in an infinite fiber-reinforced anisotropic plate containing a circular cavity with two relaxation times, *Journal of Computational and Theoretical Nanoscience* **11**: 1-7.

[11] Othman M. I. A., Hasona W.M., Abd-Elaziz E.M., 2014, Effect of rotation on micropolar generalized thermoelasticity with two temperatures using a dual-phase-lag model, *Canadian Journal of Physics* **92**: 149-158.

[12] Zenkour A. M., Abouelregal A. E., 2015, The fractional effects of a two-temperature generalized thermoelastic semi-infinite solid induced by pulsed laser heating, *Archive of Mechanics* **67**: 53-73.

[13] Biot M. A., 1956, Thermoelasticity and irreversible thermodynamics, *Journal of Applied Physics* **27**: 240-253.

[14] Lord H. W., Shulman Y., 1967, A generalized dynamical theory of thermoelasticity, *Journal Mechanics Physics of Solid* **15**: 299-309.

[15] Green A. E., Lindsay K. A., 1972, Thermoelasticity, *Journal of Elasticity* **2**: 1-7.

[16] Hetnarski R. B., Ignaczak J., 1994, Generalized thermoelasticity: response of semi-space to a short laser pulse, *Journal of Thermal Stresses* **17**: 377-396.

[17] Green A. E., Naghdi P. M., 1991, A reexamination of the basic postulate of thermo-mechanics, *Proceedings of the Royal Society of London A* **432**: 171-194.

[18] Green A. E., Naghdi P. M., 1992, On undamped heat waves in an elastic solid, *Journal of Thermal Stresses* **15**: 253-264.

[19] Green A. E., Naghdi P. M., 1993, Thermoelasticity without energy dissipation, *Journal of Elasticity* **31**: 189-208.

[20] Tzou D.Y., 1995, A unified approach for heat conduction from macro-to micro-scales, *ASME Journal of Heat Transfer* **117**: 8-16.

[21] Chandrasekharaiah D.S., 1998, Hyperbolic thermoelasticity: a review of recent literature, *Journal of Applied Mechanics Review* **51**: 705-729.

[22] Roy Choudhuri S., 2007, On a thermoelastic three-phase-lag model, *Journal of Thermal Stresses* **30**: 231-238.

[23] Quintanilla R., Racke R., 2008, A note on stability in three-phase-lag heat conduction, *International Journal of Heat and Mass Transfer* **51**: 24-29.

[24] Kar A., Kanoria M., 2009, Generalized thermo-visco-elastic problem of a spherical shell with three-phase-lag effect, *Journal of Applied Mathematical Modelling* **33**: 3287-3298.

[25] Quintanilla R., 2009, Spatial behaviour of solutions of the three-phase-lag heat equation, *Journal of Applied Mathematics and Computation* **213**: 153-162.

[26] Abbas I. A., 2014, Three-phase-lag model on thermoelastic interaction in an unbounded fiber-reinforced anisotropic medium with a cylindrical cavity, *Journal of Computational and Theoretical Nanoscience* **11**: 987-992.

[27] Othman M. I. A., Said S.M., 2014, 2D problem of magneto-thermoelasticity fiber-reinforced medium under temperature dependent properties with three-phase-lag model, *Journal of Meccanica* **49**: 1225-1241.

[28] Kumar A., Kumar R., 2015, A domain of influence theorem for thermoelasticity with three-phase-lag model, *Journal of Thermal Stresses* **38**: 744-755.
[29] Noda N., 1986, *Thermal Stresses in Materials with Temperature-Dependent Properties*, North-Holland, Amsterdam.
[30] Jin Z. H., Batra R.C., 1998, Thermal fracture of ceramics with temperature-dependent properties, *Journal of Thermal Stresses* **21**: 157-176.
[31] Othman M. I. A., 2002, Lord-Shulman theory under the dependence of the modulus of elasticity on the reference temperature in two dimensional generalized thermoelasticity, *Journal of Thermal Stresses* **25**: 1027-1045.
[32] Othman M. I. A., Song Y., 2008, Reflection of magneto-thermoelastic waves with two relaxation times and temperature dependent elastic moduli, *Journal of Applied Mathematical Modelling* **32**: 483-500.
[33] Othman M. I. A., Lotfy Kh., Farouk R. M., 2010, Generalized thermo-micro-stretch elastic medium with temperature dependent properties for different theories, *Engineering Analysis Boundary Elements* **34**: 229-237.
[34] Othman M. I. A., Elmaklizi Y. D., Said S. M., 2013, Generalized thermoelastic medium with temperature dependent properties for different theories under the effect of gravity Field, *International Journal of Thermophysics* **34**: 521-553.
[35] Wang Y. Z., Liu D., Wang Q., Zhou J. Z., 2015, Fractional order theory of thermoelasticity for elastic medium with variable material properties, *Journal of Thermal Stresses* **38**: 665-676.
[36] Belfield A. J., Rogers T. G., Spencer A. J. M., 1983, Stress in elastic plates reinforced by fibers lying in concentric circles, *Journal Mechanics Physics of Solid* **31**: 25-54.
[37] Montanaro A., 1999, On singular surface in isotropic linear thermoelasticity with initial Stress, *The Journal of the Acoustical Society of America* **106**: 1586-1588.